Journal of Ceramic Processing Research. Vol. 13, No. 3, pp. 272~277 (2012)

J O U R N A L O F
Ceramic Processing Research

The effect of milling time on the properties of binderless nanostuctured (W,Ti)C consolidated by pulsed current activated sintering

In-Jin Shon[a,*], Kwon-Il Na[a], Wonbaek Kim[b], Jae-Won Lim[b], Jung-Mann Doh[c] and Jin-Kook Yoon[c]

[a]*Division of Advanced Materials Engineering and the Research Center of Advanced Materials Development, Engineering College, Chonbuk National University, 561-756, Republic of Korea*

[b]*Minerals and Materials Processing Division, Korea Institute of Geoscience, Mining and Materials Resources, Daejeon, Republic of Korea*

[c]*Advanced Functional Materials Research Center, Korea Institute of Science and Technology, PO Box 131, Cheongryang, Seoul 130-650, Republic of Korea*

The grain size of (Ti, W)C decreases with an increase in ball milling time. Nanopowder of (Ti, W)C was fabricated by high energy ball milling for 10 h. The rapid sintering of nanostuctured (Ti, W)C hard materials was investigated with pulsed current activated sintering via a heating sintering process. The advantage of this process is that it allows very quick densification to near theoretical density and prohibition of grain growth in nanostuctured materials. A dense nanostructured (Ti,W)C hard material with a relative density of up to 99% was produced with simultaneous application of 80 MPa pressure and a pulsed current of 2700A within 3 minutes. The effect of ball milling time on the sintering behavior, grain size and mechanical properties of binderless (Ti,W)C was investigated.

Key words: Nanomaterial, Sintering, Mechanical properties, Hard material.

Introduction

Refractory metal carbides are promising ceramic materials, because these compounds exhibit unusual com-binations of physical and chemical properties such as high hardness, high melting point and excellent resistance to oxidation [1]. Industrial applications of the carbides are in cutting tools and hard coatings. Furthermore, due to their optical, electronic and magnetic properties, the carbides have been used for optical coatings, electrical contacts and diffusion barriers [2]. Among these carbides, the attractive properties of TiC and WC are a high hardness and relatively high thermal and electrical conductivities. TiC and WC also have a high chemical stability, with melting temperatures of 2727 K and 3058 K, and they do not undergo phase transformations. They are used extensively in cutting tools and abrasive materials in composites with a binder metal, such as Co or Ni. The binder phase has inferior chemical characteristics compared to the carbide phase. Most notably, corrosion and oxidation occur preferentially in the binder phase [3]. Hence, the development of binderless metal carbides is needed for water jet nozzles, mechanical seals and sliding parts due to their enhanced corrosion resistance and hardness.

*Corresponding author:
Tel : +82 63 270 2381
Fax: +82 63 270 2386
E-mail: ijshon@chonbuk.ac.kr

Nanocrystalline materials have received much attention as advanced engineering materials with improved physical and mechanical properties [4]. Since nanomaterials possess high strength, high hardness, excellent ductility and toughness, undoubtedly, more attention has been paid to the application of nanomaterials [5~7]. In recent days, nanocrystalline powders have been developed by the thermochemical and thermomechanical process named the spray conversion process (SCP), co-precipitation and high energy milling [8~10]. However, the grain size in sintered materials becomes much larger than that in pre-sintered powders due to the rapid grain growth during a con-ventional sintering process. Therefore, although the initial particle size is less than 100 nm, the grain size increases rapidly up to 500 nm or larger during conven-tional sintering [11]. So, controlling grain growth during sintering is one of the keys to the commercial success of nanostructured materials. In this regard, pulsed current activated sintering (PCAS) which can make dense materials within 2 minutes has been shown to be effective in achieving this goal [12, 13].

In this study, we investigated the sintering of (W,Ti)C without the use of a binder by the PCAS method. The goal of this research is to produce nanopowder and dense binderless nanostructured (W,Ti)C hard material. In addition, we also studied the effect of high energy ball milling on the sintering behavior and mechanical properties of binderless (W,Ti)C.

Experimental procedures

The (W,Ti)C powder with a grain size of < 1 μm and 99% purity used in this research was supplied by H.C. Starck. The powder was first milled in a high-energy ball mill (Pulverisette-5 planetary mill) at 250 rpm for various time periods (0, 1, 4, 10 h). Tungsten carbide balls (9 mm in diameter) were used in a sealed cylindrical stainless steel vial under an argon atmosphere. The weight ratio of balls-to-powder was 30:1. Milling resulted in a significant reduction in grain size. The grain size of the (W,Ti)C was calculated from the full width at half-maximum (FWHM) of the diffraction peak by Suryanarayana and Grant Norton's formula [14].

$$B_r(B_{crystalline}+B_{strain})cos\theta = k\lambda/L+\eta sin\theta \quad (1)$$

where B_r is the full width at half-maximum (FWHM) of the diffraction peak after instrumental correction; $B_{crystalline}$ and B_{strain} are the FWHM caused by the small grain size and internal stress, respectively; k is a constant (with a value of 0.9); λ is the wavelength of the X-ray radiation; L and η are the grain size and internal strain, respectively; and θ is the Bragg angle. The parameters B and B_r follow Cauchy's form with the relationship: $B = B_r + B_s$, where B and B_s are the FWHM of the broadened Bragg peaks and the standard sample's Bragg peaks, respectively.

The powders were placed in a graphite die (outside diameter, 45 mm; inside diameter, 20 mm; height, 40 mm) and then introduced into the pulsed current activated sintering (PCAS) apparatus shown schematically in Fig. 1. The PCAS apparatus includes a 30 kW power supply which provides a pulsed current (on time; 20 μs, off time; 10 μs) through the sample, and a 50 kN uniaxial load. The system was first evacuated and a uniaxial pressure of 80 MPa was applied. A pulsed current was then activated and maintained until the densification rate was negligible, as indicated by the real-time output of the shrinkage of the sample. The shrinkage was measured by a linear gauge measuring the vertical displacement. Temperatures were measured by a pyrometer focused on the surface of the graphite die. At the end of the process, the induced current was turned off and the sample cooled to room temperature. The process was carried out under a vacuum of 4×10^{-2} Torr (5.33 Pa).

The relative density of the sintered sample was measured by the Archimedes method. Microstructural information was obtained from product samples, which had been polished and etched using Murakami's reagent (10 g potassium ferricyanide, 10 g NaOH, and 100 ml water) for 1-2 minutes at room temperature. Compositional and microstructural analyses of the products were made through X-ray diffraction (XRD), scanning electron microscopy (SEM) with energy dispersive X-ray spectroscopy (EDS) and a field emission scanning electron microscope (FE-SEM). Vickers hardness was measured by performing inden-tations at a load of 10 kg_f and a dwell time of 15s.

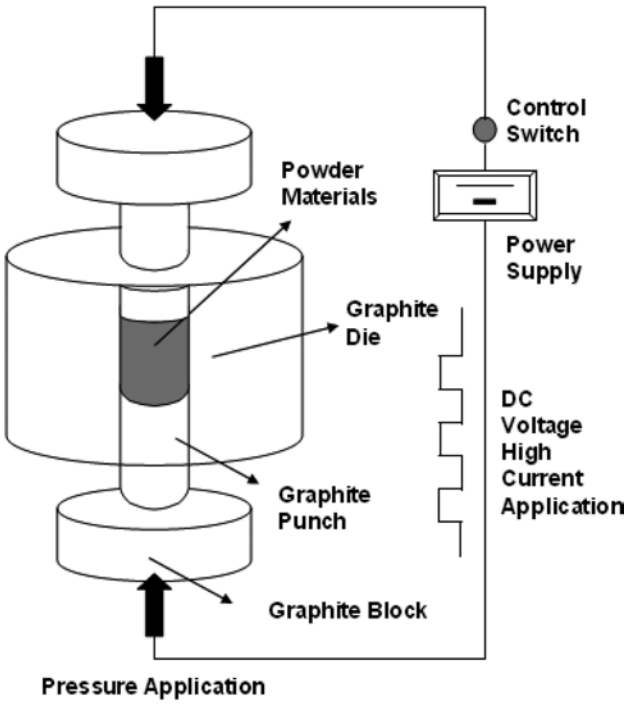

Fig. 1. Schematic diagram of the apparatus for pulsed current activated sintering.

Results and discussion

Fig. 2 shows X-ray diffraction patterns of the (W,Ti)C powder after various milling times. The full width at half-maximum (FWHM) of a diffraction peak is wider with the milling time due to strain and refinement of the powder. SEM images of the (W,Ti)C powder with milling time are shown in Fig. 3. (W,Ti)C powder decreases with increase in milling time The grain

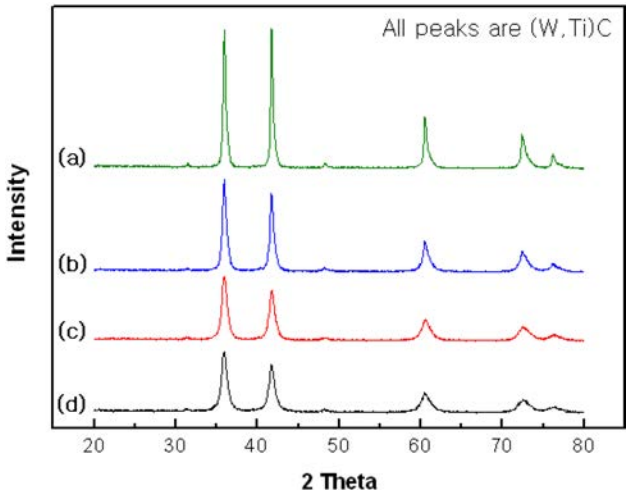

Fig. 2. X-ray diffraction patterns of the (W,Ti)C powder after various milling times : (a) 0, (b) 1, (c) 4, and (d) 10 h.

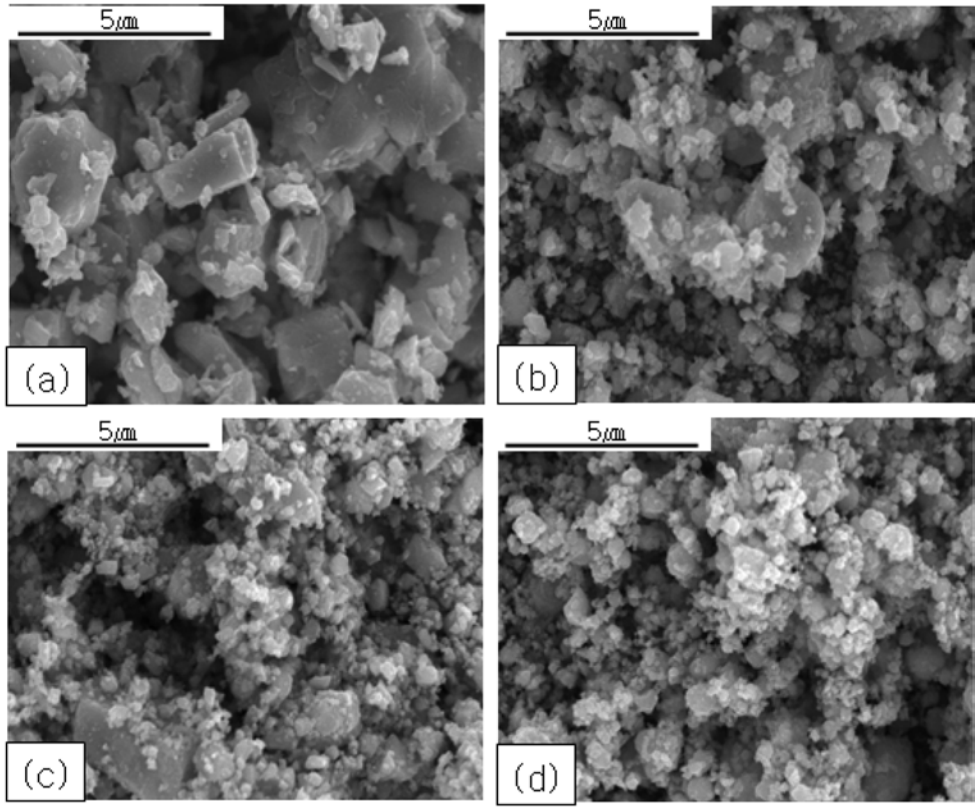

Fig. 3. TEM images of the (W,Ti)C powders with milling times : (a) 0, (b) 1, (c) 4, and (d) 10 h.

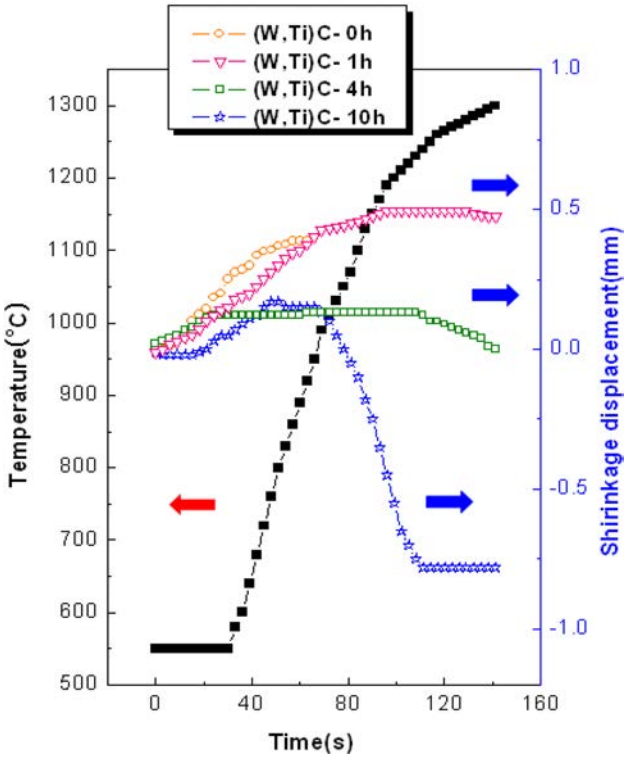

Fig. 4. Variations of temperature and shrinkage with heating time during the pulsed current activated sintering of binderless (W,Ti)C with milling times of 0, 1, 4, and 10 h.

sizes of (W,Ti)C powder milled for 1, 4, 10 h determined by Suryanarayana and Grant Norton's formula were 47, 24, and 20 nm, respectively. The variations of the shrinkage displacement and temperature with the heating time for a pulsed current 2700A during the sintering of the high energy ball milled (W,Ti)C under a pressure of 80 MPa are shown in Fig. 4. In all cases, the thermal expansion shows as soon as a pulsed current is applied. However, in the case of powder milled for 10 h the shrinkage abruptly increases at about 1000 °C. The temperature at which shrinkage started decreased with an increase in the milling time, and the high energy ball milling affected the rate of densification and the final density, as will be discussed below. A high-energy ball milling treatment allows the control of the formation of the compound by fixing the reactant powder microstructure. Indeed, high-energy ball milling produces finer crystallites, more strain and defects. Therefore, the consolidation temperature decreases with milling time because the driving force for sintering and contact points of powders for atomic diffusion increases. Fig. 5 shows SEM images of (W,Ti)C sintered from powders milled for various times and a FE-SEM image of (W,Ti)C sintered from the 10 h milled powder is shown in Fig. 6. From the figures, it is known that the (W,Ti)C is consisted of nanoparticle. And in EDS W, Ti and C peaks are detected. Fig. 7 shows the XRD patterns of (W,Ti)C sintered for all four powders used in this study. All peaks are from (W,Ti)C.

Plots of B_r ($B_{crystalline}$+B_{strain}) cosθ versus sinθ in Suryanarayana and Grant Norton's formula [14] are

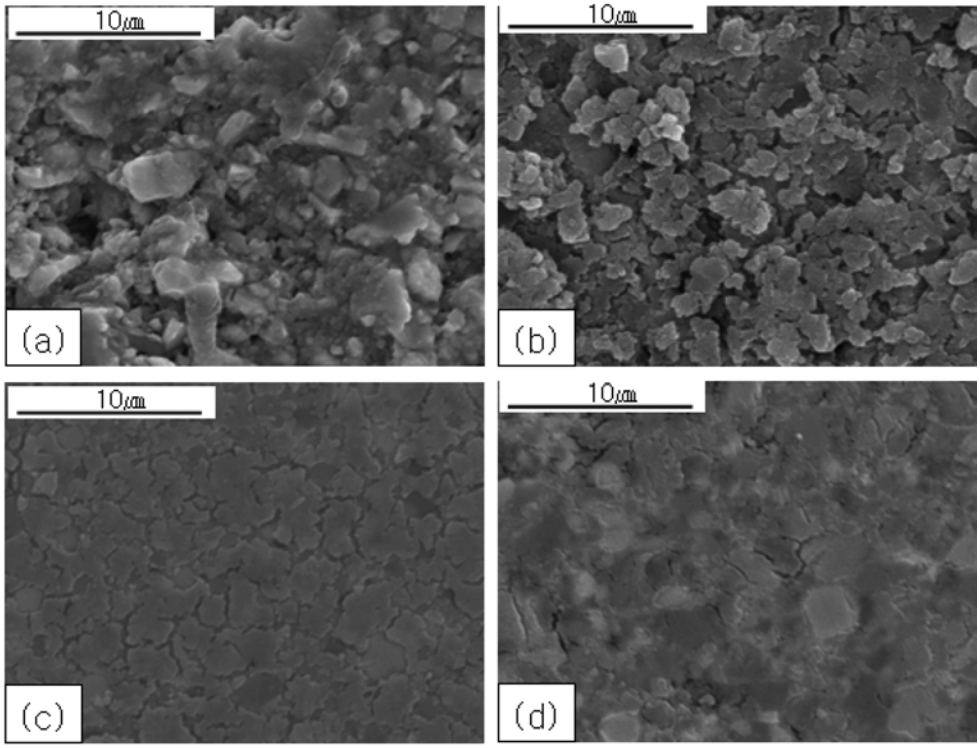

Fig. 5. SEM images of pure (W,Ti)C sintered from powder milled for : (a) 0, (b) 1, (c) 4, and (d) 10 h.

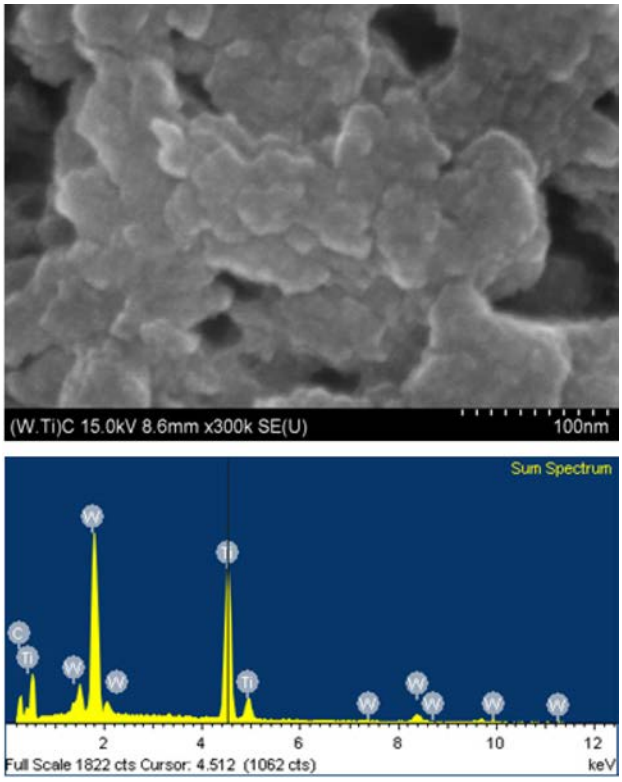

Fig. 6. FE-SEM micrograph of pure (W,Ti)C sintered from the 10 h milled powder.

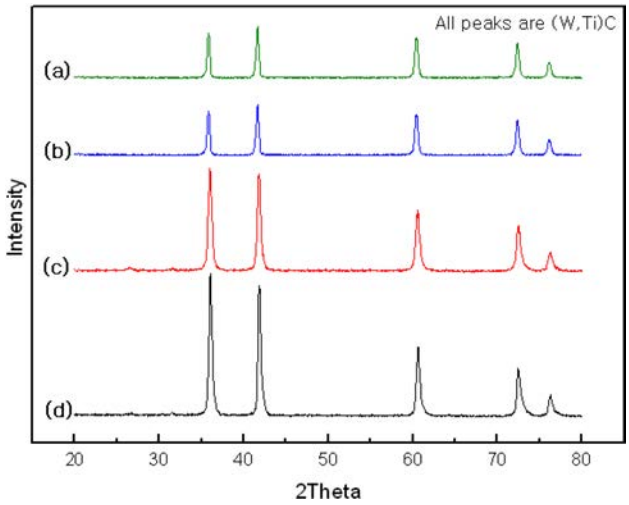

Fig. 7. XRD patterns of binderless (W,Ti)C sintered from various milled powders : (a) 0, (b) 1, (c) 4, and (d) 10 h.

shown in Fig. 8. The average grain sizes of the (W,Ti)C calculated from the XRD data were about 424, 116, 84 and 40 nm for the samples with milling times of 0, 1, 4, and 10 h and their corresponding densities were approximately 68, 78, 84 and 99%, respectively. Thus, the average grain size of the sintered (W,Ti)C is not greatly larger than that of the initial powder, indicating the absence of much grain growth during sintering. This retention of the grain size is attributed to the high heating rate and the relatively short term exposure of the powders to the high temperature.

The role of the current (resistive or inductive) in sintering has been the focus of several attempts aimed at providing an explanation of the observed enhancement of sintering and the improved characteristics of the products. The role played by the current has been variously

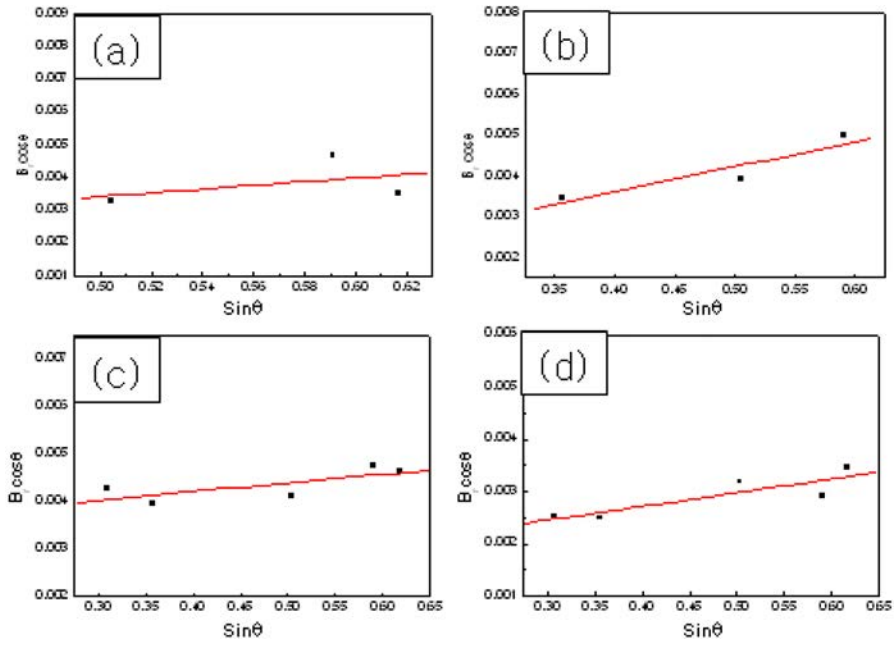

Fig. 8. Plots of B_r ($B_{crystallite} + B_{strain}$) cosθ versus sinθ for (W,Ti)C sintered from powders milled for : (a) 0, (b) 1, (c) 4, and (d) 10 h.

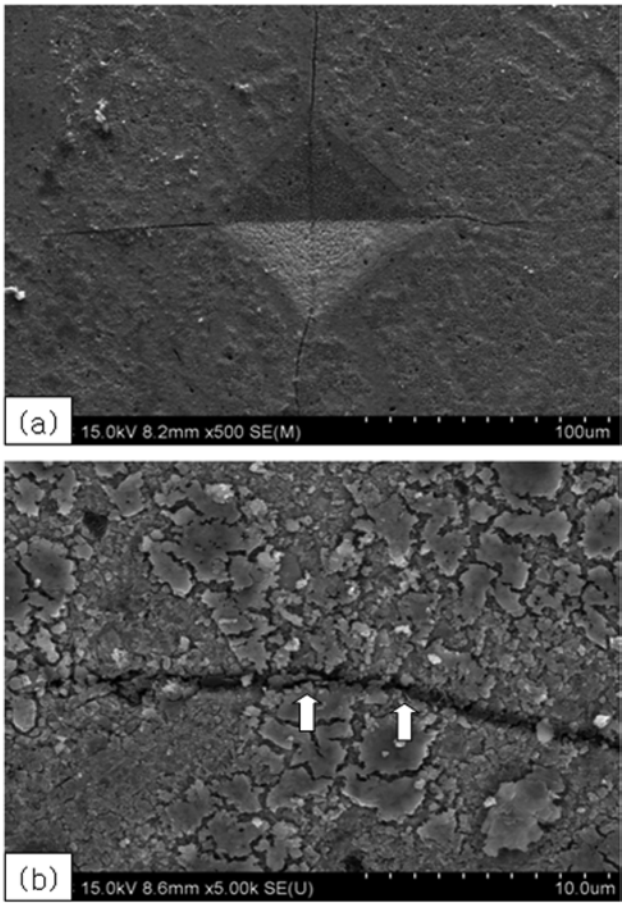

Fig. 9. (a) Vickers hardness indentation and (b) median crack propagating of the (Ti,W)C sintered from powder milled for 10h.

interpreted, the effect being explained in terms of a fast heating rate due to Joule heating, the presence of a plasma in pores separating powder particles, and the intrinsic contribution of the current to mass transport [15-18].

Vickers hardness measurements were performed on polished sections of the (W,Ti)C samples using a 10 kg_f load and 15s dwell time. Indentations with large enough loads produced radial cracks emanating from the corners of the indent. The lengths of these cracks permit estimation of the fracture toughness of the materials by means of the expression [19]:

$$K_{IC} = 0.203(c/a)^{-3/2} \cdot H_v \cdot a^{1/2} \quad (2)$$

where c is the trace length of the crack measured from the center of the indentation, a is one half of the average length of the two indent diagonals, and H_v is the hardness.

The Vickers hardnesses of the (W,Ti)C with ball milling for 4 and 10 h were 1460 $kg \cdot mm^{-2}$ and 2660 $kg \cdot mm^{-2}$, and their fracture toughnesses were 8 $MPa \cdot m^{1/2}$ and 7.5 $MPa \cdot m^{1/2}$, respectively. These values represent the average of five measurements. A higher magnification view of the indentation median crack in a (W,Ti)C sample is shown in Figure 9(b), which shows that the crack propagated deflectively (↑). The hardness of (W,Ti)C with ball milling for 10 h is very high with a high fracture toughness due to refinement of the grain structure.

Summary

Nanopowder of (W,Ti)C was fabricated by high energy ball milling. Using the rapid sintering method, PCAS, the densification of binderless (W,Ti)C was accomplished using high energy ball milling. The consolidation temperature decreased with milling time because the driving force for sintering and contact points of powders for atomic diffusion increased. The

average grain sizes of the (W,Ti)C were about 424, 116, 84 and 40 nm for the samples with milling times of 0, 1, 4, and 10 h and their corresponding densities were approximately 68. 78, 84 and 99%, respectively. The Vickers hardnesses of the (W,Ti)C with ball milling for 4 and 10 h were 1460 $kg{\cdot}mm^{-2}$ and 2660 $kg{\cdot}mm^{-2}$, and their fracture toughnesses were 8 $MPa{\cdot}m^{1/2}$ and 7.5 $MPa{\cdot}m^{1/2}$, respectively.

Acknowledgements

This study was supported by a grant from basic research project of Korea Institute of Geoscience and Mineral Resources and by the Human Resources Development of the Korea Institute of Energy Technology Evaluation and Planning (KETEP) grant funded by the Korea government Ministry of Knowledge Economy (No. 20114030200060).

References

1. O.Yu. Khyzhun, E.A. Zhurakovsky, A.K. Sinelnichenko, V.A. Kolyagin, J. Electron Spectrosc. Relat. Phenom. **82**, (1996) 179-185.
2. S.T. Oyama, Introduction to the chemistry of transition metal carbides and nitrides in : S.T. Oyama (Ed.), Blackie Academic and Professional (1996).
3. H. Suzuki, Cemented Carbide and Sintered Hard Materials, Maruzen, Tokyo, (1986) pp.62.
4. M. Sherif El-Eskandarany, J. Alloys & Compounds **305**, (2000) 225-230.
5. L. Fu, LH. Cao, Fan YS, Scripta Materialia **44**, (2001) 1061-1065.
6. K. Niihara, A. Nikahira, Advanced structural Inorganic Composite, Elsevier Scientific Publishing Co., Trieste, Italy, (1990).
7. S. Berger, R. Porat, R. Rosen, Progress in Materials **42**, (1997) 311-322.
8. Z. Fang, JW. Eason, Int. J. of Refractory Met. & Hard Mater. **13**, (1995) 297-302.
9. Wonbaek Kim, Na-Ri Kim, In-Yong Ko, Sung-Wook Cho, Je-Shin Park, In-Jin Shon, Metals and Materials International **17**, (2011) 239-243.
10. In-Yong Ko, In-Jin Shon, Jung-Mann Doh, Jin-Kook Yoon, Sang-whan Park, Na-Ra Park, J. Ceramic Processing Research **12**, (2011) 70-73.
11. M. Sommer, WD. Schubert, E. Zobetz, P. Warbichler, Int. J. of Refractory Met. & Hard Mater. **20**, (2002) 41-46.
12. Hyun-Su Kang, In-Yong Ko, Jin-Kook Yoon, Jung-Mann Doh, Kyung-Tae Hong, In-Jin Shon, Metals and Materials International **17**, (2011) 57-62.
13. S.K Bae, I.J. shon, J.M doh, J.K. Yoon, I.Y. Ko, Scripta Materialia **58**, (2008) 425-429.
14. C.Suryanarayana, M.Grant Norton, X-ray Diffraction A Practical Approach, Plenum Press, New York, (1998).
15. Z. Shen, M. Johnsson, Z. Zhao and M. Nygren, J. Am. Ceram. Soc. **85**, (2002) 1921-1927.
16. J.E. Garay, U. Anselmi-Tamburini, Z.A. Munir, S.C. Glade and P. Asoka- Kumar, Appl. Phys. Lett. **85**, (2004) 573-577.
17. J.R. Friedman, J.E. Garay. U. Anselmi-Tamburini and Z.A. Munir, Intermetallics. **12**, (2004) 589-596.
18. J.E. Garay, J.E. Garay. U. Anselmi-Tamburini and Z.A. Munir, Acta Mater., **51**, (2003) 4487-4493.
19. K. Niihara, R. Morena, and D.P.H. Hasselman, J. Mater. Sci. Lett., **1**, (1982) 12-16.